A Novel World-to-Digital-Microfluidic Interface Enabling Extraction and Purification of RNA from Human Whole Blood.

ARTICLE *in* ANALYTICAL CHEMISTRY · JANUARY 2014

Impact Factor: 5.64 · DOI: 10.1021/ac404085p · Source: PubMed

9 AUTHORS, INCLUDING:

Mais Jebrail
Sandia National Laboratories
19 PUBLICATIONS **494** CITATIONS
SEE PROFILE

Anupama Sinha
Sandia National Lab
15 PUBLICATIONS **228** CITATIONS
SEE PROFILE

Ronald F Renzi
Sandia National Laboratories
41 PUBLICATIONS **447** CITATIONS
SEE PROFILE

Steven S Branda
Sandia National Laboratories
40 PUBLICATIONS **2,427** CITATIONS
SEE PROFILE

analytical chemistry

Article

pubs.acs.org/ac

World-to-Digital-Microfluidic Interface Enabling Extraction and Purification of RNA from Human Whole Blood

Mais J. Jebrail,[†] Anupama Sinha,[‡] Samantha Vellucci,[†,⊥] Ronald F. Renzi,[§] Cesar Ambriz,[†,¶] Carmen Gondhalekar,[†,∥] Joseph S. Schoeniger,[‡] Kamlesh D. Patel,[§] and Steven S. Branda*[,†]

[†]Departments of Biotechnology and Bioengineering, [‡]Systems Biology, and [§]Advanced Systems Engineering and Deployment, Sandia National Laboratories, Livermore, California, United States

Supporting Information

ABSTRACT: Digital microfluidics (DMF) is a powerful technique for simple and precise manipulation of microscale droplets of fluid. This technique enables processing and analysis of a wide variety of samples and reagents and has proven useful in a broad range of chemical, biological, and medical applications. Handling of "real-world" samples has been a challenge, however, because typically their volumes are greater than those easily accommodated by DMF devices and contain analytes of interest at low concentration. To address this challenge, we have developed a novel "world-to-DMF" interface in which an integrated companion module drives the large-volume sample through a 10 μL droplet region on the DMF device, enabling magnet-mediated recovery of bead-bound analytes onto the device as they pass through the region. To demonstrate its utility, we use this system for extraction of RNA from human whole blood lysates (110−380 μL) and further purification in microscale volumes (5−15 μL) on the DMF device itself. Processing by the system was >2-fold faster and consumed 12-fold less reagents, yet produced RNA yields and quality fully comparable to conventional preparations and supporting qRT-PCR and RNA-Seq analyses. The world-to-DMF system is designed for flexibility in accommodating different sample types and volumes, as well as for facile integration of additional modules to enable execution of more complex protocols for sample processing and analysis. As the first technology of its kind, this innovation represents an important step forward for DMF, further enhancing its utility for a wide range of applications.

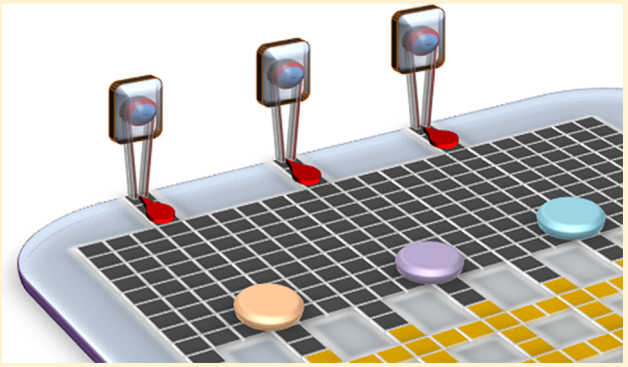

Microfluidics-based technologies have proven useful in a wide variety of applications. While microfluidic manipulations are typically carried out using microchannels, an alternative paradigm has recently emerged, called digital microfluidics (DMF).[1] In DMF, discrete nanoliter- to microliter-sized droplets of fluid are manipulated on a planar hydrophobic surface by applying a series of electrical potentials to an array of electrode pads.[2,3] DMF has rapidly become popular for chemical, biological, and medical applications,[4] as it allows straightforward control over multiple reagents (no pumps, valves, or tubing required),[5−7] facile handling of both solids and liquids (no channels to clog),[8−10] and compatibility with even troublesome reagents (e.g., organic solvents, corrosive chemicals) because the hydrophobic surface (typically Teflon-coated) is chemically inert.[11,12] However, a continuing challenge for DMF is handling of "real-world" samples, which typically are composed of fluid volumes greater than those easily accommodated by DMF devices, containing analytes of interest at concentrations too dilute to support downstream processing and detection without prior concentration. Our group[13−15] and others[16−18] have demonstrated that droplets can be dispensed onto DMF devices from large volumes (hundreds of microliters to milliliters) contained in off-device reservoirs; this only partially addresses the challenge, however, because on-device processing of hundreds or thousands of droplets to collect enough analyte for further manipulation is often not a realistic strategy. Off-device concentration prior to introduction into the DMF device can be a good solution for reagents,[19] because generally they are prepared in large batches for use in hundreds or thousands of reactions. However, off-device concentration of sample analytes must be carried out independently for each sample, necessitating considerable manual labor (or a robotic system) and risking contamination of, and worker exposure to, the samples. In-line concentration of sample analytes for further manipulation in the DMF device is a better solution but to date has not been achieved.

In answer to this challenge, we have developed a novel "world-to-DMF" interface in which an integrated companion module repeatedly drives the entirety of a large-volume sample through a 10 μL droplet region on the DMF device, enabling

Received: December 12, 2013
Accepted: January 30, 2014

dx.doi.org/10.1021/ac404085p | *Anal. Chem.* XXXX, XXX, XXX−XXX

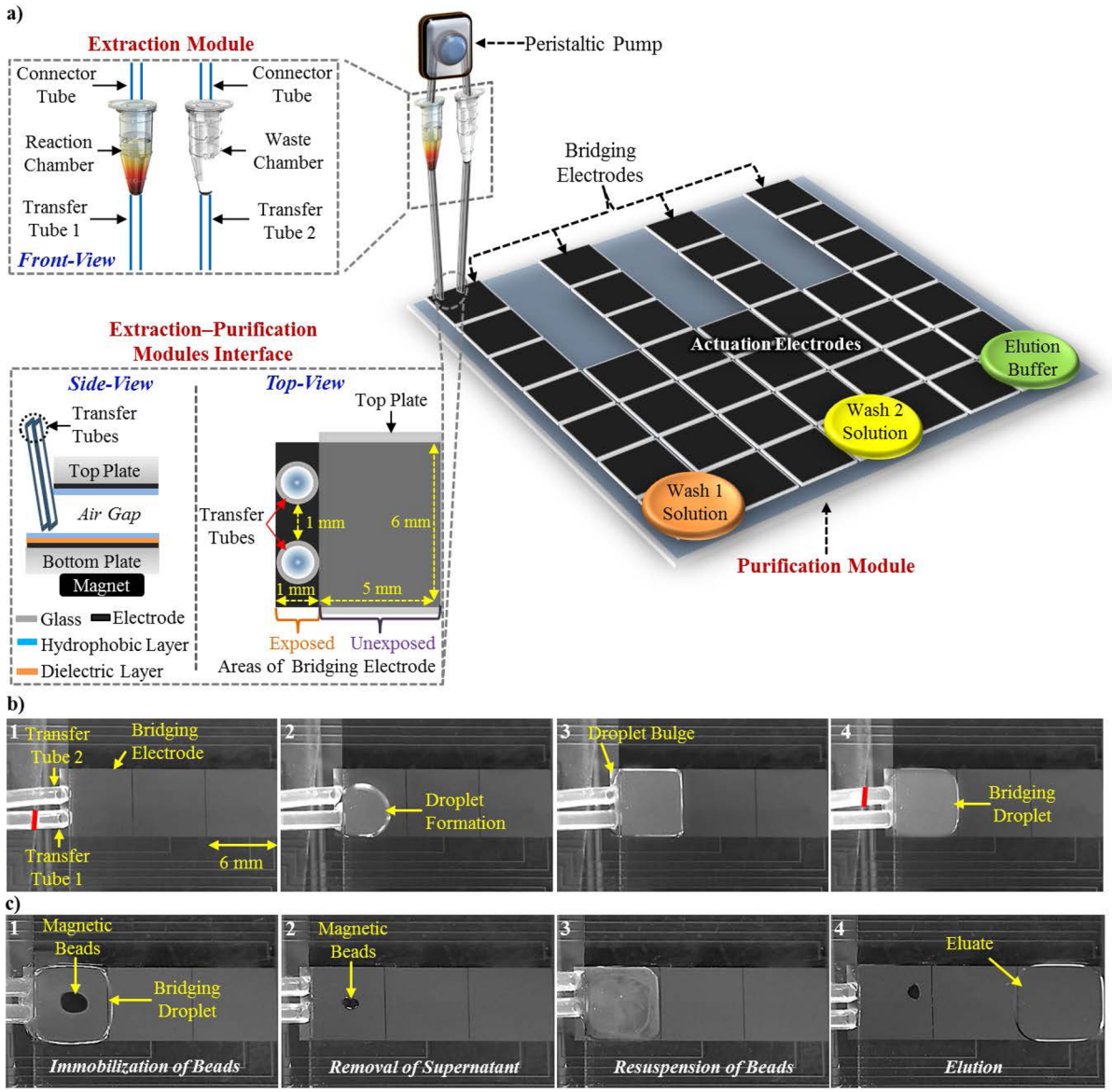

Figure 1. World-to-digital microfluidics (DMF) system. (a) Top- and side-view of system, which is composed of an Extraction Module, a DMF-based Purification Module, and fluidic integration at their interface via a Bridging Droplet. A movable magnet located beneath the Bridging Electrode enables immobilization and release of analyte-binding magnetic beads within the Bridging Droplet. (b) Stills from a video (top-view) showing formation of the Bridging Droplet (10 μL). Red lines indicate the air/liquid interface within Transfer Tubes (frames 1 and 4). (c) Stills from a video (top-view) showing magnetic bead-based steps in analyte purification. Beads in a macroscale volume (500 μL) are flowed through the Bridging Droplet and immobilized upon the Bridging Electrode surface via engagement of the magnet beneath (frame 1). The supernatant is sent to waste (frame 2), and the beads are resuspended in a droplet of Elution Buffer (10 μL) upon disengagement of the magnet (frame 3). Finally, the beads are reimmobilized, and the eluate is recovered (frame 4).

magnet-mediated recovery of bead-bound analytes onto the device as they pass through the region. To demonstrate the utility of this system, RNA was extracted from human whole blood lysates (110−380 μL) and further purified in microscale volumes (5−15 μL) in the DMF device itself. Processing by the system was >2-fold faster and consumed 12-fold less reagents yet produced RNA yields and quality fully comparable to conventional preparations. The system is designed for facile reconfiguration and reprogramming, for accommodation of a wide variety of sample types and volumes. As the first technology of its kind, this innovation represents an important step forward for DMF, further enhancing its utility for a wide range of applications.

EXPERIMENTAL SECTION

Reagents and Materials. Fluorinert FC-40, Pluronic F127, ethanol, and isopropanol were purchased from Sigma Chemical (St. Louis MO); MagMAX-Blood RNA Isolation Kits from Life Technologies (Grand Island NY); Parylene C dimer from Specialty Coating Systems (Indianapolis IN); and Teflon-AF from DuPont (Wilmington DE). Whole blood specimens from healthy volunteer donors were collected by and purchased from ProMedDx (Norton MA). MagMAX kit working solutions were prepared according to the manufacturer's instructions, while also adding Pluronic F127 (0.1% w/v)[20] to the Elution Buffer.

System Assembly and Operation. Assembly and operation of the world-to-DMF system are described here in

dx.doi.org/10.1021/ac404085p | Anal. Chem. XXXX, XXX, XXX−XXX

brief; more comprehesive and detailed descriptions can be found in the Supporting Information section.

The Extraction Module was composed of two 500 μL microcentrifuge tubes (Reaction and Waste Chambers, respectively), each fitted with a Connector Tube (interface with peristaltic pump) and a Transfer Tube (interface with Purification Module) (Figure 1a). The Purification Module was composed of a DMF device fabricated in-house. The bottom DMF plate, bearing 40 patterned chromium electrode pads (6 × 6 mm, with 40 μm interelectrode gaps), was formed by photolithography and etching.[21] A 7 μm layer of Parylene-C plate was added via vapor deposition and a 50 nm layer of Teflon-AF via spin-coating. The top plate (glass coated with unpatterned indium tin oxide) was spin-coated with 50 nm of Teflon-AF. The plates were assembled with a spacer consisting of three pieces of double-sided tape (total thickness of 300 μm), offsetting their lateral alignment to expose 1 mm of the Bridging Electrode on the bottom plate. An adjustable magnetic stand positioned the Extraction Module such that its Transfer Tubes made contact with the Bridging Electrode at an ∼70° angle, and a custom-made spacing manifold was used to maintain this interaction.

Transfer Tube 1 was preloaded with Lysis Solution (65, 130, or 260 μL) and RNA Binding Beads (20 μL), separated by a 20 μL air gap (Figure S-1a, Supporting Information). The Purification Module was preloaded with Wash 1 Solution (15 μL), Wash 2 Solution (15 μL), and Elution Buffer (10 μL). The blood specimen (25, 50, or 100 μL) was introduced into the Reaction Chamber via pipetting. Then, the Lysis Solution was aspirated into the Reaction Chamber and actively mixed with the blood by shuttling the bolus between Transfer Tube 1 and the Reaction Chamber for 30 s. The RNA Binding Beads were aspirated into the Reaction Chamber and mixed with the blood lysate for 30 s, and the mixture (total volume: 110, 200, or 380 μL) was left to stand for an additional 5 min. After 30 s of mixing, the pump was directed to simultaneously dispense from Transfer Tube 1 and aspirate into Transfer Tube 2, and at the same time, voltage was applied to the Bridging Electrode. This combination of forces caused: (1) expulsion of the bolus from Transfer Tube 1 onto the Bridging Electrode; (2) growth and swelling of the droplet, as energization of the electrode pad prevented spread beyond its boundaries; (3) contact between the droplet and Transfer Tube 2, creating a continuous fluid stream between the two Transfer Tubes (a 10 μL "Bridging Droplet"); and (4) uptake of fluid by Transfer Tube 2 (see Figure 1b and Supporting Information video ac404085-p_si_003.wmv "Bridging Droplet Formation"). The RNA Binding Beads were then collected by immobilizing them on the Bridging Electrode using a magnet positioned directly beneath it while shuttling the bolus between the Transfer Tubes (via the Bridging Droplet) (Figure 1c). After sending the fluid to the Waste Chamber, the Wash 1 Solution droplet was driven onto the Bridging Electrode (actuating this and other droplets in the Purification Module via application of voltage to adjacent electrode pads[3]). After shuttling the beads-containing droplet between the Transfer Tubes to mix, the magnet was re-engaged to recover the beads, and the fluid sent to the Waste Chamber. This sequence was repeated using the Wash 2 Solution droplet and then the Elution Buffer droplet, in the last step sending the RNA-containing eluate to a recovery site within the Purification Module for collection via pipetting and off-device analyses.

Conventional RNA Preparation. Each whole blood specimen (25, 50, or 100 μL) was mixed with Lysis Solution (65, 130, or 260 μL) in a microcentrifuge tube via pipetting, and the lystate was incubated at RT for 2 min. RNA Binding Beads (20 μL) were added to the lysate and, after vortexing, the mixture was incubated at RT for 5 min. The reaction tube was then placed upon a magnetic stand (Life Technologies, Grand Island NY), immobilizing the beads against the tube wall in order to enable removal of the supernatant via pipetting. The beads were washed twice with Wash 1 Solution (150 μL) and once with Wash 2 Solution (150 μL), in each case resuspending them by removing the tube from the magnetic stand and vortexing, then reimmobilizing them prior to removal of the supernatant. Finally, they were resuspended in Elution Buffer (30 μL), incubated at RT for 2 min, and reimmobilized for recovery of the RNA-containing eluate.

RNA Analysis. RNA yield and purity (A_{260}/A_{280}) were measured using a NanoDrop 2000 UV−vis spectrophotometer (Thermo Scientific, Wilmington DE) or a Qubit 2.0 fluorometer (Life Technologies, Carlsbad CA). Fragment size distribution and RNA integrity number (RIN) were obtained using an RNA 6000 Pico Chip on a 2100 Bioanalyzer (Agilent, Santa Clara CA).

For qRT-PCR analysis, total RNA prepared from 50 μL of human whole blood was used as template for first-strand cDNA synthesis by SuperScript III RT (Life Technologies, Carlsbad CA), following the manufacturer's recommendations. The first-strand cDNA products, in turn, were used as template for qPCR targeting beta-2-microglobulin (B2M), glyceraldehyde 3-phosphate dehydrogenase (GAPDH), and peptidylpropyl isomerase B (PPIB), using Taqman reagents (Life Technologies, Carlsbad CA) in combination with SsoFast Probes Supermix (BioRad, Hercules CA). Four independent qPCR experiments were carried out for each of the three targets, and the reactions within each experiment were carried out in triplicate.

For RNA-Seq analysis, total RNA prepared from 50 μL of human whole blood was used as template in Peregrine cDNA library preparation reactions.[22] Hydroxyapatite (HAC) mediated molecular normalization of the libraries, to selectively deplete highly abundant transcripts (primarily rRNA), was carried out as previously described.[23] Library yields were measured using a Qubit 2.0 fluorometer (Life Technologies, Carlsbad CA), and fragment size distribution was obtained using a High Sensitivity DNA Assay Chip on a 2100 Bioanalyzer (Agilent, Santa Clara CA). The individually barcoded libraries were mixed together in equal ratios, and the final concentration of the multiplexed library was measured using Kapa qPCR (Kapa Biosystems, Woburn MA). The multiplexed library was loaded into a MiSeq SGS machine (Illumina, San Diego CA), at 15 pM concentration, for a 50 bp single-end run. The SGS run was repeated once with the same multiplexed library, to account for run-to-run variability. Raw FASTQ sequence files were demultiplexed using MiSeq Reporter (Illumina, San Diego CA) and processed with a custom quality filter perl script (qfilter.pl).[22] High-quality reads were mapped to the human genome using TopHat[24] (version 2.0.94) with default parameters and second-strand alignment against the UCSC hg19 assembly. Cufflinks[25] (version 2.1.1) was used to estimate transcript abundance [i.e., fragments per kilobase of exon model per million mapped reads (FPKM)] and to assess sample-to-sample variability. Plots of Log_{10} FPKM

dx.doi.org/10.1021/ac404085p | Anal. Chem. XXXX, XXX, XXX−XXX

values were created using *Mathematica* 9.0.1 (Wolfram Research, Champaign IL).

RESULTS AND DISCUSSION

System Design and Operation. As shown in Figure 1a, our world-to-DMF system consists of three distinct components: An Extraction Module, which enables macroscale extraction of RNA from blood; a Purification Module, which enables microscale purification and concentration of the RNA; and a Module Interface, which mediates interaction between the modules to enable transition from the macroscale to the microscale. The Extraction Module is composed of a Reaction Chamber; a Waste Chamber; a pair of Connector Tubes, for coupling the Chambers to a single peristaltic pump; and a pair of Transfer Tubes, which conduct fluids from the Chambers to the Module Interface and vice versa. Fluids are delivered through pressure-driven flow generated by the pump. The Purification Module consists of a DMF device in which fluid droplets are sandwiched between a bottom plate bearing an array of working electrode pads and a top plate that serves as the counter electrode; droplets are actuated by applying voltage to adjacent positions to generate electrowetting forces.[2,3] A key feature of the Purification Module is the Bridging Electrode: A working electrode pad is located at the periphery of the device and only partially covered by the top plate, such that the pad's external edge (~1 mm × 6 mm) is left exposed and accessible. The Module Interface primarily consists of the Bridging Droplet, which is formed upon the Bridging Electrode. The Bridging Droplet fluidically integrates the Extraction Module (via its Transfer Tubes) with the Purification Module, providing the means by which the macroscale (Extraction Module) to microscale (Purification Module) transition is achieved in a straightforward fashion (no adhesives, fittings, etc.).

Fluidic integration of the system is depicted in Figure 1b and demonstrated in Supporting Information video ac404085-p_si_003.wmv "Bridging Droplet Formation". First, the peristaltic pump is directed to drive a fluid bolus from the Reaction Chamber into Transfer Tube 1 (Figure 1b, frame 1). As the bolus nears the distal end of Transfer Tube 1, the Bridging Electrode is activated (AC potential: 100 V_{rms}). This generates an electrowetting force that further encourages transfer of the bolus from Transfer Tube 1 to the Bridging Electrode (frame 2) and holds the newly formed droplet in place, preventing its spread to neighboring electrodes. With further flow from Transfer Tube 1, the droplet grows to fully cover the Bridging Electrode and then begins to swell, eventually making contact with the distal end of Transfer Tube 2 (frame 3). By directing the pump to aspirate fluid into Transfer Tube 2 while continuing to dispense fluid from Transfer Tube 1, the Bridging Droplet is formed (frame 4) and fluidic integration of the system is achieved. In this way, a macroscale volume from the Extraction Module is routed through a microscale volume in the Purification Module (the 10 μL Bridging Droplet) and returned to the Extraction Module. Analytes of interest are collected from the macroscale volume into the Bridging Droplet, enabling their manipulation in microscale volumes within the Purification Module; thus, the world-to-DMF transition is accomplished.

In developing the world-to-DMF interface, three strategies were implemented for achieving reliable formation of the Bridging Droplet. The first is related to adjusting the surface tension of fluids dispensed into the air-gap between the bottom and top plates of the Purification Module. In initial experiments, we found that fluids with high surface tension (e.g., water) resisted entry into the air-gap, whereas fluids supplemented with ≥15% of organic solvents[26,27] (e.g., ethanol or isopropanol) readily entered the air-gap and remained suspended between the bottom and top plates due to surface tension. The second strategy concerns the lateral alignment of the top plate relative to the bottom plate. In initial experiments, conventional lateral alignment of the plates (i.e., squared off so that the top plate fully covered the bottom plate) failed to provide the Transfer Tubes with sufficient access to the Bridging Electrode for reliable formation of the Bridging Droplet. In our final design, the edge of the top plate is recessed to expose ~1 mm of the Bridging Electrode on the bottom plate, as depicted in Figure 1a; this enables the Transfer Tubes to directly access the Bridging Electrode from above, greatly improving the consistency with which the Bridging Droplet is formed. The third strategy addresses the choreography of fluid movements required for formation of the Bridging Droplet. We found that coordination of several fluid-driving forces, dispensation from Transfer Tube 1, aspiration into Transfer Tube 2, and actuation of the Bridging Electrode, was essential for tightly controlled formation of the Bridging Droplet. Implementing these three strategies in combination has enabled precise and consistent formation of the Bridging Droplet, which is necessary for the success of our world-to-DMF interface.

Example Application: Blood RNA Extraction and Purification. To evaluate the utility of our world-to-DMF system in processing of real-world samples, we tasked it with extraction and purification of total RNA from human whole blood specimens, through implementation of a magnetic bead-based protocol.[28] We focused on blood specimens of 25−100 μL because this volume range is typical for "fingerstick" capillary sampling, which is convenient (e.g., no phlebotomist required), inexpensive, and commonly used in a variety of clinical, field, and research settings.[29−34] As illustrated in Figure S-1a, Supporting Information, a blood specimen (25, 50, or 100 μL) was introduced into the system's Reaction Chamber and then sequentially mixed with Lysis Solution (65, 130, or 260 μL) and RNA Binding Beads (20 μL), in each case aspirating the preloaded reagent from Transfer Tube 1 into the Reaction Chamber and then rapidly shuttling the bolus between the two locations to mix thoroughly. After allowing the beads to bind RNA in the lysate (5 min incubation), the reaction mixture (total volume: 110, 200, or 380 μL) was passed through the Bridging Droplet (10 μL) (Figure S-1b, frame 1, Supporting Information) three times while engaging an external magnet beneath the Bridging Droplet, such that the beads were recovered from the reaction mixture by immobilizing them on the surface of the Bridging Electrode (frame 2). The reaction mixture fluid was aspirated into the Waste Chamber, and the Bridging Droplet was reconstituted using 15 μL of Wash 1 Solution delivered to the Bridging Electrode by the Purification Module via electrowetting (frame 3). The beads were released into this new Bridging Droplet (by disengaging the magnet), and the fluid shuttled between Transfer Tubes 1 and 2 in order to thoroughly wash the bead-bound RNA (demonstrated in Supporting Information video ac404085p_si_004.wmv "Magnetic Bead Mixing"). After recovering the beads onto the surface of the Bridging Electrode (by re-engaging the magnet) and sending the fluid to the Waste Chamber, the wash cycle was repeated using 15 μL of Wash 2 Solution (frame 4). Finally, the cycle was repeated using 10 μL of Elution Buffer

dx.doi.org/10.1021/ac404085p | *Anal. Chem.* XXXX, XXX, XXX−XXX

(frame 5), in the last step sending the RNA-containing fluid to a recovery site in the Purification Module.

The world-to-DMF system offers several advantages relative to conventional methods for RNA extraction and purification, including faster processing times (20 versus 45 min) and reduced consumption of reagents (12-fold). These advantages are conferred by limiting most sample processing steps to the confines of microscale volumes (5−15 μL) within the DMF device, which enables rapid and (through interaction with the Extraction Module) highly efficient perfusion of bead-bound RNA using small volumes of reagents. Moreover, the automated and precise control of different reagents,[11] volumes,[35] and phases[8,12] (e.g., fluids versus beads) afforded by DMF simplifies the sample processing protocol (no need for vortex mixers, magnetic stands, orbital shakers, etc.), and in-line concentration of sample analytes (as opposed to off-device concentration prior to introduction into the DMF device) reduces risk of contaminating, and/or exposing workers to, the samples.

Evaluation of System Performance. We evaluated the performance of our world-to-DMF system by comparing its processing products to those generated by conventional extraction and purification of blood RNA. We found that the two approaches generated similar RNA yields from 25 or 50 μL of blood, with the world-to-DMF system giving slightly better yields from 100 μL of blood (Figure 2a). The latter effect may reflect a greater efficiency in capturing "free" RNA from the large volume, owing to pressure-driven convective transport[36] of the lysate through the pile of magnetic beads during their immobilization upon the surface of the Bridging Electrode (whereas only diffusive transport is at work in the conventional method). In any case, all of the blood RNA yields were within the range typically reported in the literature.[34,37] The RNA preparations also closely resembled one another with regard to their size distribution profiles, with each characterized by a broad range of RNA sizes as well as prominent abundance peaks at sizes corresponding to the 28S and 18S rRNA (Figures 2b and S-2, Supporting Information). RNA purity (A_{260}/A_{280} ratio) and integrity (RNA integrity number; RIN) measurements indicated that all of the RNA preparations were of comparably high quality (Table S-1, Supporting Information).[37,38] Thus, by standard metrics, the physical properties of processing products from the world-to-DMF system were essentially indistinguishable from those generated by conventional extraction and purification of blood RNA.

Despite these indications of its high quality, it was important to confirm that the blood RNA prepared by the world-to-DMF system was capable of supporting complex enzymatic reactions, such as those routinely used in analyzing transcriptional activity. To this end, blood RNA samples prepared by the world-to-DMF system were first tested for their ability to serve as template in qRT-PCR reactions. We found that these RNA samples fully supported qRT-PCR analysis of gene expression, as demonstrated through measurement of relative levels of transcripts from three representative ("housekeeping") genes (Figure 3). For each of the genes analyzed, qRT-PCR using world-to-DMF versus conventionally prepared blood RNA as template generated expression level (threshold cycle; C_t) measurements that were essentially identical regardless of template source. qRT-PCR analysis of RNA prepared by the world-to-DMF system generated slightly higher C_t values on average, but the difference was not statistically significant ($p \geq 0.07$). In all cases, the measured expression levels were comparable to literature values.[39,40]

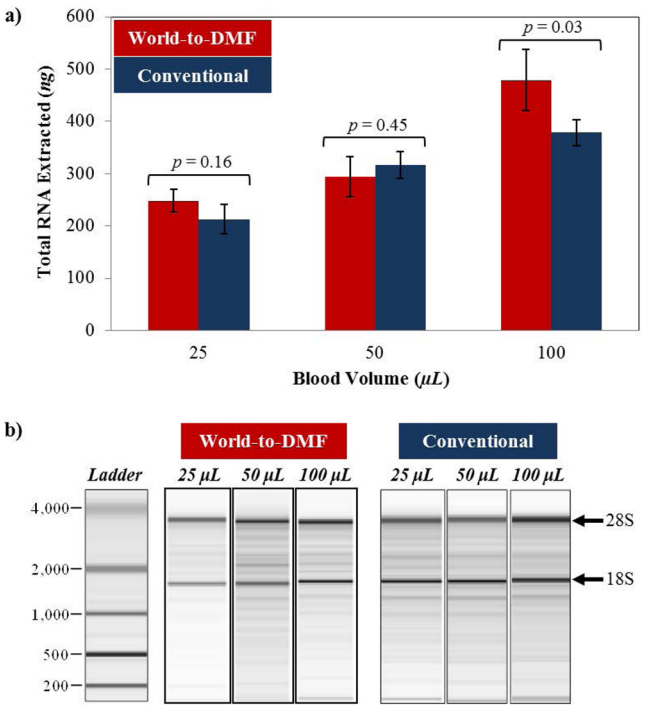

Figure 2. Characterization of total RNA extracted and purified from human whole blood using the world-to-DMF system. (a) Yields of total RNA purified from different volumes of human blood (25, 50, and 100 μL) using the world-to-DMF system (red) or conventional preparation (blue). Bars indicate the mean ± standard deviation of three RNA preparations for each condition. *P* values were calculated using Student's *t*-test (unpaired, two-tailed, unequal variances). (b) Fragment size distributions in blood RNA samples produced by the world-to-DMF system (red) or conventional preparation (blue). Size distribution profiles were generated through Bioanalyzer analysis; the 28S and 18s rRNA bands are indicated.

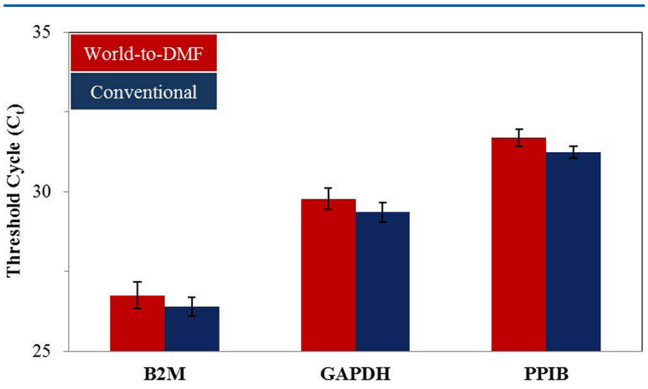

Figure 3. qRT-PCR analysis of total RNA extracted and purified from human whole blood using the world-to-DMF system. Total RNA was prepared from 50 μL aliquots of whole blood from three different human donors, using either the world-to-DMF system (red) or the conventional approach (blue). Each RNA sample served as template in four independent qRT-PCR experiments for each of three targets (B2M, GAPDH, and PPIB), and the reactions within each experiment were carried out in triplicate. Bars indicate the mean ± standard deviation for the three RNA samples. *P* values were calculated using Student's *t*-test (unpaired, two-tailed, unequal variances).

dx.doi.org/10.1021/ac404085p | *Anal. Chem.* XXXX, XXX, XXX−XXX

As a further test of their utility, blood RNA samples prepared by the world-to-DMF system were used as template in generating cDNA libraries for global transcriptional profiling via Second Generation Sequencing (SGS) (i.e., RNA-Seq). We found that cDNA yields (Table S-2, Supporting Information) and size distribution profiles (Figure S-3, Supporting Information) were similar to those of libraries generated using RNA conventionally prepared from the same blood specimens. In all cases, sequencing of the libraries generated reads of high quality (95−96% passed Qfilter) that successfully mapped to the reference human genome (~99%) (Table S-2, Supporting Information). Direct comparison of the transcriptional profiles represented in libraries derived from world-to-DMF versus conventionally prepared RNA revealed a high degree of similarity [coefficient of determination (R^2) values of ~0.85] (Table S-2 and Figures 4 and S-4, Supporting Information), indicating that no strong bias was imposed by the RNA preparation method.

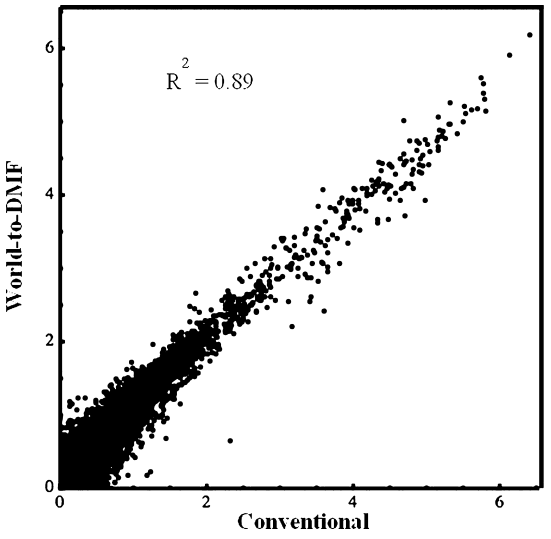

Figure 4. RNA-Seq analysis of total RNA extracted and purified from human whole blood using the world-to-DMF system. Total RNA was prepared from 50 μL aliquots of whole blood from three different human donors, using either the world-to-DMF system or the conventional approach. Each RNA sample served as template in generating a cDNA library for Second Generation Sequencing (SGS). After depleting highly abundant sequences (primarily rRNA) through molecular normalization, the six individually barcoded libraries were mixed together in equal ratios, and the multiplexed library was loaded into a MiSeq sequencer for a 50 bp single-end run. High-quality reads were mapped to the reference human genome, and transcript abundance [i.e., fragments per kilobase of exon model per million mapped reads (FPKM)] was calculated for each of the genes "hit". The scatter plot shows the Log_{10} FPKM value for each gene, as measured using RNA prepared from a representative blood specimen (blood specimen 1) by the world-to-DMF system versus the conventional approach. The overall similarity of the FPKM profiles is indicated by the coefficient of determination (R^2) value.

In summary, these results indicate that blood RNA samples prepared by our world-to-DMF system are of high quality and fully compatible with two analytical methods routinely used for gene expression studies: qRT-PCR and RNA-Seq. The fact that the RNA samples successfully served as template for these PCR-based methods indicates that the world-to-DMF system is able to eliminate or inactivate PCR inhibitors present in blood specimens[41−43] and strongly suggests that its processing products will prove to be suitable for other PCR-based analytical methods as well. The high quality of its products, comparable to that of benchscale preparations, further suggests that they will similarly support non-PCR-based analytical methods, such as Northern blot, RNase protection, electrophoretic mobility shift, and coprecipitation analyses.

CONCLUSIONS

We have developed a novel (and, to our knowledge, the first) engineered system for collecting target analytes from a macroscale sample and efficiently transferring them to a DMF device for further manipulation in microscale volumes. This world-to-DMF system enabled us to recover high-quality RNA from human blood specimens (25−100 μL), through macroscale extraction of blood lysates (110−380 μL) followed by microscale purification of their RNA (5−15 μL). World-to-DMF system processing was >2-fold faster and consumed 12-fold less reagents yet produced RNA yields and quality fully comparable to conventional preparations. In its current format, the system supports processing of single blood specimens; by incorporating multiple peristaltic pumps and multiple/larger DMF devices, it should be straightforward to construct a system capable of processing dozens, and perhaps hundreds, of specimens in parallel. Similarly, the system could be reconfigured for extraction of multi-mL specimens (by increasing the dimensions of Extraction Module components) and/or for purification of sub-μL samples (by reducing the dimensions of Purification Module features, particularly the distance separating the DMF plates and the surface area of each electrode pad).[2] Additionally, with modest modification to reaction conditions, the system should prove useful in processing a wide variety of specimens (clinical, environmental) and analytes (nucleic acids, proteins, metabolites, viruses, cells). Moreover, current and future configurations of the system should support complex downstream processing and analysis, carried out by the DMF device itself[5,14,44−47] and/or additional microfluidics-based modules that are fluidically integrated with the DMF device.[13,46,48]

ASSOCIATED CONTENT

Supporting Information

Additional information as noted in text. This material is available free of charge via the Internet at http://pubs.acs.org.

AUTHOR INFORMATION

Corresponding Author

*E-mail: sbranda@sandia.gov. Tel: +1 925 294 6751. Fax: +1 925 294 3020.

Present Addresses

[⊥]S.V.: Stratos Genomics, Seattle, Washington, United States.
[¶]C.A.: Stanford University, Stanford, California, United States.
[‖]C.G.: Oregon State University, Corvallis, Oregon, United States.

Notes

The authors declare no competing financial interest.

ACKNOWLEDGMENTS

The authors thank Harrison Edwards, Jim Van De Vreugde, and Mark R. Claudnic for their contributions to the design and fabrication of our DMF devices. This work was funded by the Sandia National Laboratories (SNL) Laboratory-Directed

Research and Development (LDRD) program (grant 158814). SNL is a multiprogram laboratory managed and operated by Sandia Corporation, a wholly owned subsidiary of Lockheed Martin Corporation, for the U.S. Department of Energy's National Nuclear Security Administration under contract DE-AC04-94AL85000.

REFERENCES

(1) Wheeler, A. R. *Science* **2008**, *322*, 539−540.
(2) Pollack, M. G.; Fair, R. B.; Shenderov, A. D. *Appl. Phys. Lett.* **2000**, *77*, 1725−1726.
(3) Lee, J.; Moon, H.; Fowler, J.; Schoellhammer, T.; Kim, C. J. *Sens. Actuators, A: Phys.* **2002**, *95*, 259−268.
(4) Jebrail, M. J.; Bartsch, M. S.; Patel, K. D. *Lab Chip* **2012**, *12*, 2452−2463.
(5) Hua, Z.; Rouse, J. L.; Eckhardt, A. E.; Srinivasan, V.; Pamula, V. K.; Schell, W. A.; Benton, J. L.; Mitchell, T. G.; Pollack, M. G. *Anal. Chem.* **2010**, *82*, 2310−2316.
(6) Choi, K.; Ng, A. H. C.; Fobel, R.; Wheeler, A. R. *Annu. Rev. Anal. Chem.* **2012**, *5*, 413−440.
(7) Jebrail, M. J.; Ng, A. H. C.; Rai, V.; Hili, R.; Yudin, A. K.; Wheeler, A. R. *Angew. Chem., Int. Ed.* **2010**, *49*, 8625−8629.
(8) Jebrail, M. J.; Yang, H.; Mudrik, J. M.; Lafreniere, N. M.; McRoberts, C.; Al-Dirbashi, O. Y.; Fisher, L.; Chakraborty, P.; Wheeler, A. R. *Lab Chip* **2011**, *11*, 3218−3224.
(9) Mousa, N. A.; Jebrail, M. J.; Yang, H.; Abdelgawad, M.; Metalnikov, P.; Chen, J.; Wheeler, A. R.; Casper, R. F. *Sci. Transl. Med.* **2009**, *1*, 1ra2.
(10) Yang, H.; Mudrik, J. M.; Jebrail, M. J.; Wheeler, A. R. *Anal. Chem.* **2011**, *83*, 3824−3830.
(11) Chatterjee, D.; Hetayothin, B.; Wheeler, A. R.; King, D. J.; Garrell, R. L. *Lab Chip* **2006**, *6*, 199−206.
(12) Jebrail, M. J.; Wheeler, A. R. *Anal. Chem.* **2009**, *81*, 330−335.
(13) Sinha, A.; Jebrail, M. J.; Kim, H.; Patel, K. D.; Branda, S. S. *J. Visualized Exp.* **2013**, No. e50597.
(14) Kim, H.; Jebrail, M. J.; Sinha, A.; Bent, Z. W.; Solberg, O. D.; Williams, K. P.; Langevin, S. A.; Renzi, R. F.; Van De Vreugde, J. L.; Meagher, R. J.; Schoeniger, J. S.; Lane, T. W.; Branda, S. S.; Bartsch, M. S.; Patel, K. D. *PLoS One* **2013**, *8*, No. e68988.
(15) Kim, H.; Bartsch, M. S.; Renzi, R. F.; He, J.; Van de Vreugde, J. L.; Claudnic, M. R.; Patel, K. D. *J. Lab. Autom.* **2011**, *16*, 405−414.
(16) Shah, G. J.; Ding, H.; Sadeghi, S.; Chen, S.; Kim, C. J.; van Dam, R. M. *Lab Chip* **2013**, *13*, 2785−2795.
(17) Ding, H.; Sadeghi, S.; Shah, G. J.; Chen, S.; Keng, P. Y.; Kim, C. J.; van Dam, R. M. *Lab Chip* **2012**, *12*, 3331−3340.
(18) Ren, H.; Fair, R. B.; Pollack, M. G. *Sens. Actuators, B: Chem.* **2004**, *98*, 319−327.
(19) Yang, H.; Luk, V. N.; Abeigawad, M.; Barbulovic-Nad, I.; Wheeler, A. R. *Anal. Chem.* **2009**, *81*, 1061−1067.
(20) Luk, V. N.; Mo, G. C. H.; Wheeler, A. R. *Langmuir* **2008**, *24*, 6382−6389.
(21) Jebrail, M. J.; Luk, V. N.; Shih, S. C. C.; Fobel, R.; Ng, A. H. C.; Yang, H.; Freire, S. L. S.; Wheeler, A. R. *J. Visualized Exp.* **2009**, No. e1603.
(22) Langevin, S. A.; Bent, Z. W.; Solberg, O. D.; Curtis, D. J.; Lane, P. D.; Williams, K. P.; Schoeniger, J. S.; Sinha, A.; Lane, T. W.; Branda, S. S. *RNA Biol.* **2013**, *10*, 502−515.
(23) Vandernoot, V. A.; Langevin, S. A.; Solberg, O. D.; Lane, P. D.; Curtis, D. J.; Bent, Z. W.; Williams, K. P.; Patel, K. D.; Schoeniger, J. S.; Branda, S. S.; Lane, T. W. *BioTechniques* **2012**, *53*, 373−380.
(24) Rodrigue, S.; Materna, A. C.; Timberlake, S. C.; Blackburn, M. C.; Malmstrom, R. R.; Alm, E. J.; Chisholm, S. W. *PLoS One* **2010**, *5*, No. e11840, DOI: 10.1371/journal.pone.0011840.
(25) Trapnell, C.; Williams, B. A.; Pertea, G.; Mortazavi, A.; Kwan, G.; van Baren, M. J.; Salzberg, S. L.; Wold, B. J.; Pachter, L. *Nat. Biotechnol.* **2010**, *28*, 511−515.
(26) Kirby, A. E.; Wheeler, A. R. *Lab Chip* **2013**, *13*, 2533−2540.
(27) Dow, G. J. Method for wetting a powder containing benzoyl peroxide. United States of America patent, WO2011049547 A1 (Apr 28, 2011).
(28) *MagMAX-96 Blood RNA Isolation Kit (User Guide)*, September 2012, http://tools.invitrogen.com/content/sfs/manuals/cms_055422.pdf (accessed 20 August 2013).
(29) Garty, G.; Karam, A.; Brenner, D. J. *Int. J. Radiat. Biol.* **2011**, *87*, 754−765.
(30) Hack, C. M.; Scarfi, C. A.; Sivitz, A. B.; Rosen, M. D. *Pediatr. Emerg. Care* **2013**, *29*, 319−323.
(31) Loewenstein, D.; Stake, C.; Cichon, M. *Am. J. Emerg. Med.* **2013**, *31*, 1236−1239.
(32) Belardinelli, A.; Benni, M.; Tazzari, P. L.; Pagliaro, P. *Vox Sang.* **2013**, *105*, 116−120, DOI: 10.1111/vox.12033.
(33) Larrat, S.; Bourdon, C.; Baccard, M.; Garnaud, C.; Mathieu, S.; Quesada, J. L.; Signori-Schmuck, A.; Germi, R.; Blanc, M.; Leclercq, P.; Hilleret, M. N.; Leroy, V.; Zarski, J. P.; Morand, P. *J. Clin. Virol.* **2012**, *55*, 220−225.
(34) Robison, E. H.; Mondala, T. S.; Williams, A. R.; Head, S. R.; Salomon, D. R.; Kurian, S. M. *BMC Genomics* **2009**, *10*, 1471−2164.
(35) Abdelgawad, M.; Freire, S. L. S.; Yang, H.; Wheeler, A. R. *Lab Chip* **2008**, *8*, 672−677.
(36) Model, M. A.; Omann, G. M. *Biophys. J.* **1995**, *69*, 1712−1720.
(37) Menke, A.; Rex-Haffner, M.; Klengel, T.; Binder, E. B.; Mehta, D. *BMC Res. Notes* **2012**, *5*, 1756−0500.
(38) Kiewe, P.; Gueller, S.; Komor, M.; Stroux, A.; Thiel, E.; Hofmann, W. K. *Ann. Hematol.* **2009**, *88*, 1177−1183.
(39) Stamova, B. S.; Apperson, M.; Walker, W. L.; Tian, Y.; Xu, H.; Adamczy, P.; Zhan, X.; Liu, D. Z.; Ander, B. P.; Liao, I. H.; Gregg, J. P.; Turner, R. J.; Jickling, G.; Lit, L.; Sharp, F. R. *BMC Med. Genomics* **2009**, *2*, 1755−8794.
(40) Dheda, K.; Huggett, J. F.; Bustin, S. A.; Johnson, M. A.; Rook, G.; Zumla, A. *BioTechniques* **2004**, *37*, 112−114.
(41) Schrader, C.; Schielke, A.; Ellerbroek, L.; Johne, R. *J. Appl. Microbiol.* **2012**, *113*, 1014−1026.
(42) Wilson, I. G. *Appl. Environ. Microbiol.* **1997**, *63*, 3741−3751.
(43) Radstrom, P.; Knutsson, R.; Wolffs, P.; Lovenklev, M.; Lofstrom, C. *Mol. Biotechnol.* **2004**, *26*, 133−146.
(44) Malic, L.; Veres, T.; Tabrizian, M. *Lab Chip* **2009**, *9*, 473−475.
(45) Boles, D. J.; Benton, J. L.; Siew, G. J.; Levy, M. H.; Thwar, P. K.; Sandahl, M. A.; Rouse, J. L.; Perkins, L. C.; Sudarsan, A. P.; Jalili, R.; Pamula, V. K.; Srinivasan, V.; Fair, R. B.; Griffin, P. B.; Eckhardt, A. E.; Pollack, M. G. *Anal. Chem.* **2011**, *83*, 8439−8447.
(46) Thaitrong, N.; Kim, H.; Renzi, R. F.; Bartsch, M. S.; Meagher, R. J.; Patel, K. D. *Electrophoresis* **2012**, *33*, 3506−3513.
(47) Malic, L.; Veres, T.; Tabrizian, M. *Biosens. Bioelectron.* **2011**, *26*, 2053−2059.
(48) Watson, M. W. L.; Jebrail, M. J.; Wheeler, A. R. *Anal. Chem.* **2010**, *82*, 6680−6686.